



**HAL**  
open science

# Referential description of the evolution of a 2D swarm of robots interacting with the closer neighbors: Perspectives of continuum modeling via higher gradient continua

Alessandro Della Corte, Antonio Battista, Francesco Dell'Isola

## ► To cite this version:

Alessandro Della Corte, Antonio Battista, Francesco Dell'Isola. Referential description of the evolution of a 2D swarm of robots interacting with the closer neighbors: Perspectives of continuum modeling via higher gradient continua. *International Journal of Non-Linear Mechanics*, 2015, 12 p. 10.1016/j.ijnonlinmec.2015.06.016 . hal-01236021

**HAL Id: hal-01236021**

**<https://hal.science/hal-01236021>**

Submitted on 1 Dec 2015

**HAL** is a multi-disciplinary open access archive for the deposit and dissemination of scientific research documents, whether they are published or not. The documents may come from teaching and research institutions in France or abroad, or from public or private research centers.

L'archive ouverte pluridisciplinaire **HAL**, est destinée au dépôt et à la diffusion de documents scientifiques de niveau recherche, publiés ou non, émanant des établissements d'enseignement et de recherche français ou étrangers, des laboratoires publics ou privés.

# Referential description of the evolution of a 2D swarm of robots interacting with the closer neighbors: Perspectives of continuum modeling via higher gradient continua

Alessandro Della Corte <sup>a,\*</sup>, Antonio Battista <sup>d,b</sup>, Francesco dell'Isola <sup>c,b</sup>

<sup>a</sup> Doctoral School in Theoretical and Applied Mechanics, Università di Roma La Sapienza, 18 Via Eudossiana, Rome

<sup>b</sup> MeMoCS, International Research Center for the Mathematics & Mechanics of Complex Systems, Università dell'Aquila, Italy

<sup>c</sup> Department of Structural and Geotechnical Engineering, Università di Roma La Sapienza, 18 Via Eudossiana, Rome

<sup>d</sup> Department of Physics, University Federico II, Naples, Via Cinthia 1-80126, Naples, Italy

---

## A B S T R A C T

In the present paper a discrete robotic system model whose elements interact via a simple geometric law is presented and some numerical simulations are provided and discussed. The main idea of the work is to show the resemblance between the cases of first and second neighbors interaction with (respectively) first and second gradient continuous deformable bodies. Our numerical results showed indeed that the interaction and the evolution process described is suitable to closely reproduce some basic characteristics of the behavior of bodies whose deformation energy depends on first or on higher gradients of the displacement. Moreover, some specific qualitative characteristics of the continuous deformation are also reproduced. The model introduced here will need further investigation and generalization in both theoretical and numerical directions.

---

## 1. Introduction

In the literature one usually indicates, with the expression “swarm robot”, a system which is constituted by a certain number of interacting elements which behave autonomously and whose interaction is simple and rather localized (see e.g. [1,3]). The introduction of these systems was at first motivated by the desire to model the so-called “collective intelligence” of animals like ants, bees and several species of birds [2,10], or even some more elementary form of life, like *Physarum polycephalum*, a unicellular slime mold that demonstrates interesting collective intelligence (see e.g. [6–8]). In all these cases, the idea was to show that very simple interaction laws between the constituting elements can produce very complex collective behaviors, and this statement can be considered by now well-established.

As often is the case, the introduction of a new tool originated many different lines of investigation, and in the last years, swarm robots have become a very active research field, with researchers from several areas (engineering, mathematical physics, probability theory) contributing to it (useful general theoretical references are [19,4]). While the main interest of the majority of works concerning swarm robots was aimed

at studying how to prescribe a desired collective behavior controlling only few elements of the swarm (the so-called “leaders”) and at analyzing the stability of the system (the reader is referred e.g. to [5,9]), we intend here to use the swarm robot model as a numerical investigation tool. In the present work, indeed, the idea is to model a particular swarm robotic system to investigate its potential relationship with an apparently not so close subject: continuum mechanics of higher gradient deformable media, i.e. continua in which the deformation energy density depends on second and higher gradients of the displacement. Several very sound results are by now available (the reader can see e.g. [47,11,12,21,37,43]), by means of which several specific characteristics of this kind of continua have been shown and proven; moreover, homogenized continuous limit of specific discrete mechanical system can lead to higher gradient continua, and yet the current status of higher gradient theories is sometimes considered still controversial.

The introduction of discrete system as an approximation of continuous systems is of course a very important research line today, and in particular the consideration of complex real-world systems can easily lead to the necessity to consider both a continuous and a discrete part in the formal description of the same object (see e.g. [36]). The interactions which we considered in our swarm robot model were chosen thinking at their potential resemblance with the constitutive laws typically associated with higher gradient continuum models, so as to have a discrete model supporting their meaningfulness and scientific

---

\* Corresponding author.

E-mail addresses: [alessandro.dellacorte@uniroma1.it](mailto:alessandro.dellacorte@uniroma1.it) (A. Della Corte),  
[antonio.battista@studenti.unina.it](mailto:antonio.battista@studenti.unina.it) (A. Battista),  
[francesco.dellisola@uniroma1.it](mailto:francesco.dellisola@uniroma1.it) (F. dell'Isola).

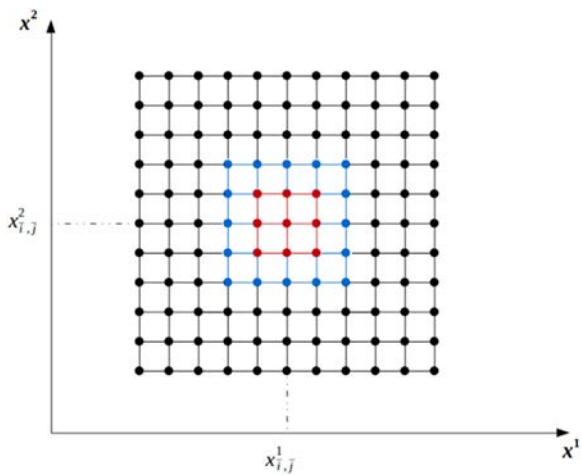


**Fig. 1.** Reference configuration  $C^0$ . In red the first neighbors and in blue the second neighbors of element  $(\bar{i}, \bar{j})$ . (For interpretation of the references to color in this figure caption, the reader is referred to the web version of this paper.)

relevance. The paper is organized as follows. In the first section, a description of the swarm robot model is provided. In the second one, the numerical results are shown, and a comparison with a 2D higher gradient continuum is provided. Finally, some conclusions and some ideas for future developments of this line of investigation are provided in the conclusions.

## 2. The model

### 2.1. Generality and first neighbors interaction

Let us consider a swarm  $\mathfrak{E}$  constituted by a finite number of elements, and indicate by  $C^0$  the reference configuration of  $\mathfrak{E}$ . In  $C^0$  the elements of  $\mathfrak{E}$  occupy all the nodes of a square grid sized  $L \times L$ . We consider a set of time steps, i.e. a set of ordered discrete values for the time variable  $t$  that we will denote with  $\mathfrak{T}_m = \{0, t_1, \dots, t_m, \dots\}$ . Let us consider an orthonormal reference system with axes that are parallel to the grid, whose unit length is equal to the side of the cell grid in  $C^0$ , and whose origin coincides with the left bottom vertex of the swarm. We indicate the (“Lagrangian”) elements of  $\mathfrak{E}$  by means of the pair of indexes  $(ij)$  characterizing their position in  $C^0$ , and by  $(x_{ij}^1, x_{ij}^2)(t_m)$  the coordinates of the element occupying the node  $(ij)$  in  $C^0$  at the time  $t_m$ . For each element  $(ij)$  in  $C^0$  we define a set  $N_n(\bar{i}, \bar{j})$  of  $n$ th neighbors by

$$N_n(\bar{i}, \bar{j}) := \{(i, j) \in C^0 : \rho[(\bar{i}, \bar{j}), (i, j)] = n\}$$

where  $\rho$  indicates the  $\mathbb{R}^2$ -Chebyshev distance.<sup>1</sup> This gives, for  $n=1$  and  $n=2$ , the definition of first and second neighbors graphically represented in Fig. 1. Note that the given concept of  $n$ -th neighbors is Lagrangian, i.e. the system keeps memory of the identity of the neighbors of a given element of  $\mathfrak{E}$ . The motivation of this choice lies in the desire to reproduce some relevant characteristics of deformable (solid) bodies, in which the behavior of constitutive particles depends on molecular interactions which are preserved (at least in absence of fractures) in the evolution of the system. This leads to some additional theoretical problems when dealing with the proof of collective properties, but is in our opinion an unavoidable choice in our selected line of investigation.

Let us select a leader, i.e. one element  $\varrho$  sitting in the node  $(\bar{i}, \bar{j})$  in  $C^0$ , to which a prescribed motion  $\mathcal{M}$  is imposed. We namely

consider a function

$$\mathcal{M} : t_m \in \mathfrak{T}_m \longrightarrow (x_{ij}^1, x_{ij}^2)(t_m) \in \mathbb{R}^2$$

which defines the actual position of  $\varrho$ .

An interaction is defined between the elements of the system in the following way. As said, let  $C^0$  be the actual configuration of the system at the time  $t_0 = 0$ . We define now a set of “virtual” configurations by means of which we will move to the “true” new configuration  $C^{t_1}$ . Let thus  $V_0^{t_1}$  be the virtual configuration in which  $\varrho$  is in  $\mathcal{M}(t_1)$  while all other elements are in the same position they had in  $C^0$ . Let us now define another virtual configuration  $V_1^{t_1}$ , in which:

1. the leader  $\varrho$  is where it was in  $V_0^{t_1}$ ;
2. every one of its first neighbor  $N_1(\bar{i}, \bar{j})$  moves to the centroid<sup>2</sup> of its own first neighbors in  $V_0^{t_1}$ ;
3. all others elements are in the same position they had in  $V_0^{t_1}$ .

Iterating the previous evolution law, let thus  $V_n^{t_1}$  be the virtual configuration in which:

1. the leader  $\varrho$  along with its first  $n-1$ -th neighbors are in the same position they had in  $V_{(n-1)}^{t_1}$ ;
2. every one of the  $n$ -th neighbors of  $\varrho$  has moved to the centroid of its own first neighbors in  $V_{(n-1)}^{t_1}$ ;
3. all others elements are in the same position they had in  $V_{(n-1)}^{t_1}$ .

When the virtual step  $n$  reaches the value of the maximum Chebyshev distance  $n = \bar{n}$  of  $\varrho$  from the boundary in  $C^0$ , we define the actual configuration  $C^{t_1}$  as  $V_{\bar{n}}^{t_1}$ . Iterating the whole evolution process we will get the actual configurations  $C^{t_1}, C^{t_1}, \dots, C^{t_m}, \dots$ . A graphical representation of the virtual configurations is shown in Fig. 2.

A specification has to be done for the previously described interaction. When the conditions 2 concern an element that belongs to the boundary, the set of the first neighbors, as defined above, has less than 8 elements, and the computation of the centroid makes less sense as it leads to undesirable edge-effects. To avoid this problem, a “fictitious” boundary is introduced in the model, i.e. a set of elements surrounding the swarm and following their closest “true” elements. More formally, the elements of the fictitious boundary have in  $C^0$  coordinates

$$\begin{aligned} &((L+1), a) \\ &(a, (L+1)) \\ &(-1, a) \\ &(a, -1) \end{aligned}$$

where  $a$  takes the values  $\{-1, \dots, (L+1)\}$  (the fictitious boundary is graphically represented in Fig. 4). To characterize the motion of the fictitious boundary, we introduce a final virtual configuration  $V_{\bar{n}}^{t_1}$ , in which no “true” element moves and the fictitious boundary elements move according to the following law:

1. A fictitious vertex element has the same displacement of the true vertex which is among its first neighbors.
2. A fictitious side element  $(-1, j)$  has the same displacement of the element  $(0, j)$ .
3. A fictitious side element  $(i, L+1)$  has the same displacement of the element  $(i, L)$ .
4. A fictitious side element  $(i, -1)$  has the same displacement of the element  $(i, 0)$ .

<sup>2</sup> By centroid of a set of points  $P_1(x_1^1, \dots, x_1^n), \dots, P_m(x_m^1, \dots, x_m^n) \in \mathbb{R}^n$  we mean of course the point  $P(\sum_{i=1}^m \frac{x_i^1}{m}, \sum_{i=1}^m \frac{x_i^2}{m}, \dots, \sum_{i=1}^m \frac{x_i^n}{m})$ .

<sup>3</sup> See below for the application of the condition 2 to boundary elements.

<sup>1</sup> By Chebyshev distance in  $\mathbb{R}^2$  one means the distance given by  $\rho((x^1, x^2), (y^1, y^2)) = \max\{|x^1 - y^1|, |x^2 - y^2|\}$ .

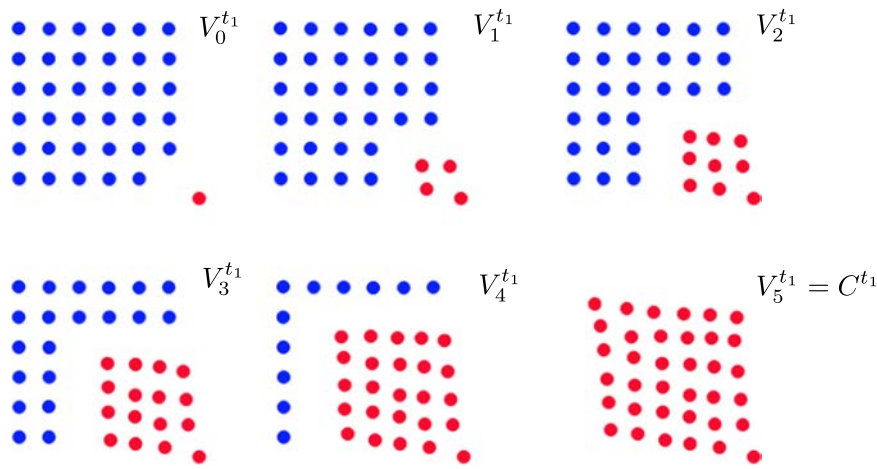


**Fig. 2.** The six pictures are relative to six virtual configurations between  $C^{t_0}$  and  $C^{t_1}$  for a  $6 \times 6$  swarm. For clarity, a displacement was introduced for the leader (bottom right corner) which is much larger, with respect to the step length, than that used in the following simulations. The elements in red are the ones which are already in the position they will have in  $C^{t_1}$ . (For interpretation of the references to color in this figure caption, the reader is referred to the web version of this paper.)

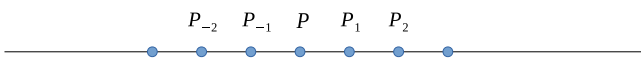


**Fig. 3.** First and second neighbors in a monodimensional discrete system.

A fictitious side element  $(L+1, j)$  has the same displacement of 5. the element  $(L, j)$ .

With this introduction, every “true” element of the swarm has exactly 8 neighbors (including the fictitious ones).

With the above described interaction law, the perturbation of the system due to the prescribed motion imposed to the leader  $\mathcal{Q}$  propagates “virtually” in succession on every square frame around  $\mathcal{Q}$ , while in every actual configuration  $C^{t_m}$  it has acted on all the elements of  $\Xi$  up to the  $m$ -th time step. This means that the effects of the perturbation caused by the imposed motion of the leader propagates instantly, but that its effects are suitably (we will see what we mean with that) weighted by the distance, so as to have critical times after which the “full” effect of the propagation reaches the farthest elements.

## 2.2. Second neighbors interaction and multiple leaders set

It is natural to extend the previously given interaction law to the second neighbors modifying the condition 2 above introduced in the following way:

2. *bis* every one of the  $n$ -th neighbors of  $\mathcal{Q}$  has moved to the centroid of its own *first and second* neighbors in  $V_{(n-1)}^{t_1}$ .<sup>4</sup>

The centroid can be computed either in a straightforward manner, i.e. just considering the simple average of the coordinates of the first and second neighbors (we will call it a “mixed interaction”), or weighting the contribution of first and second neighbors in a given way. In this last case, in particular, one can set the weight of the first neighbors at zero, so as to have what we will call a “pure second neighbor” interaction.

Dealing with a second neighbor interaction, a double fictitious boundary has to be introduced in order to have a full set of 24 first and second neighbors for every element, thus avoiding the undesirable edge-effects before mentioned. Indeed, we introduced a set of elements surrounding the swarm and having in  $C^0$

coordinates

$((L+1), a)$	$((L+2), b)$
$(a, (L+1))$	$(b, (L+2))$
$(-1, a)$	$(-2, b)$
$(a, -1)$	$(b, -2)$

where  $a$  takes the values  $\{-1, \dots, (L+1)\}$  and  $b$  takes the values  $\{-2, \dots, (L+2)\}$ . In this case, another virtual configuration  $V_{f_2}^{t_m}$  is introduced, in which no element belonging to the true set or to the first fictitious boundary moves and the fictitious boundary moves, with the elements of the second fictitious boundary moving according to the following law:

1. A fictitious vertex element has the same displacement of the first fictitious boundary vertex which is among its first neighbors.
2. A fictitious side element  $(-2, j)$  has the same displacement of the element  $(-1, j)$ .
3. A fictitious side element  $(i, L+2)$  has the same displacement of the element  $(i, L+1)$ .
4. A fictitious side element  $(i, -2)$  has the same displacement of the element  $(i, -1)$ .
5. A fictitious side element  $(L+2, j)$  has the same displacement of the element  $(L+1, j)$ .

As said, and as we will see with numerical simulations, the main idea behind the introduction of second neighbors interaction is to have a good and computationally advantageous discrete approximation of second gradient continua. A theoretical justification for this idea can be sketched as follows.

Let us start by noticing that the geometric centroid of a given set of points  $P_1, \dots, P_n$  is the point that minimizes the sum of the squared distances from the points, i.e. the function

$$f(P) = \sum_{i=1}^n \|P_i, P\|^2$$

Consequently, one can reasonably think to the continuous limit of the discrete system under the given interaction law as to a system in which the energy depends quadratically on the distance; this constitutes implicitly a justification of the physical plausibility of the proposed algorithm. Let us now consider, for simplicity, a mono-dimensional discrete system, as the one shown in Fig. 3.

It is straightforward to see that for a first-neighbors interaction, the deformation energy density (depending on squared distances

<sup>4</sup> See below for the application of the condition 2.*bis* to boundary or close-to-boundary elements.

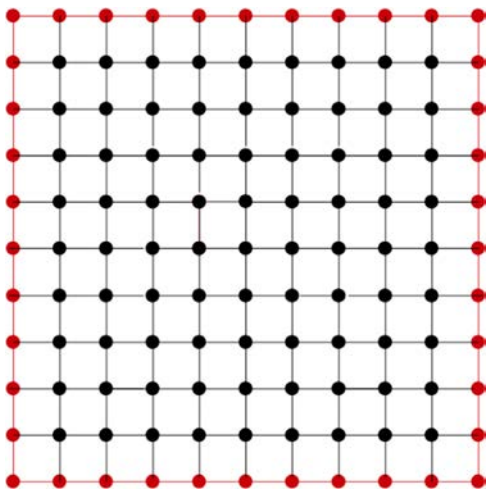


**Fig. 4.** A  $10 \times 10$  Swarm in black and the fictitious boundary in red. (For interpretation of the references to color in this figure caption, the reader is referred to the web version of this paper.)

from first neighbors) can be written as a function of first-order finite differences of the placement  $\chi$  for a given point  $P$

$$\mathcal{E}(\|P_1, P\|^2, \|P_{-1}, P\|^2) = \mathcal{E}[(\chi(P_1) - \chi(P)), (\chi(P_{-1}) - \chi(P))] = \mathcal{E}(\nabla_\epsilon \chi), \quad (1)$$

where  $\nabla_\epsilon$  indicates the finite difference with step  $\epsilon$ . With second-neighbors interaction, this is not possible (keeping the natural choice of the step of the lattice as the step length for the computation of finite differences), and instead a second gradient model is called for. In fact in this case direct computation shows

$$\begin{aligned} \mathcal{E} &= \mathcal{E}[(\chi(P_1) - \chi(P)), \dots, (\chi(P_n) - \chi(P))] \\ &= \mathcal{E}[(\chi(P_1) - \chi(P)), (\chi(P_2) - \chi(P_1)) + (\chi(P_1) - \chi(P)), (\chi(P_{-1}) - \chi(P)), \\ &\quad (\chi(P_{-2}) - \chi(P_{-1})) + (\chi(P_{-1}) - \chi(P))] \\ &= \mathcal{E}[(\chi(P_1) - \chi(P)), (\chi(P_{-1}) - \chi(P)), (\chi(P_1) - \chi(P) - (\nabla \nabla)_\epsilon^f \chi(P)), \\ &\quad (\chi(P_{-1}) - \chi(P) - (\nabla \nabla)_\epsilon^b \chi(P))] \\ &= \mathcal{E}[\nabla_\epsilon^f \chi(P), \nabla_\epsilon^b \chi(P), \nabla_\epsilon^f \chi(P) - (\nabla \nabla)_\epsilon^f \chi(P), \nabla_\epsilon^b \chi(P) - (\nabla \nabla)_\epsilon^b \chi(P)], \end{aligned}$$

where the apexes  $f$  and  $b$  indicate respectively forward and backward finite differences on the lattice. Notice that the last

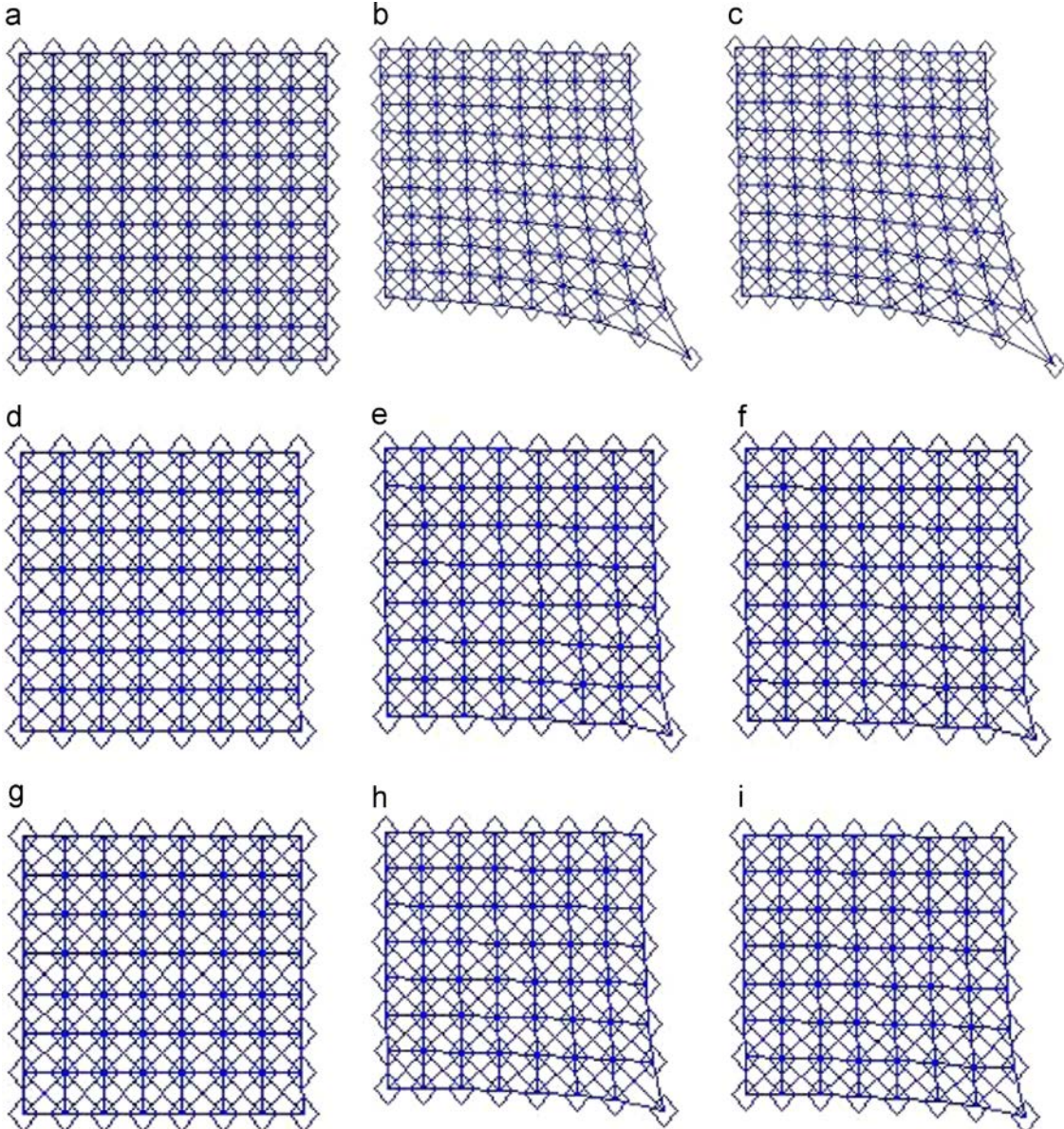


**Fig. 5.** Snapshots of the swarm at time steps  $t = 1, 500, 1000$  in the case of FNI (a,b,c), SNI (d,e,f) and MI (g,h,i), with the leader moving at velocity  $v=0.01$  length units/time step in direction  $(1, -1)$ .

expression for the energy, though not involving central second finite differences, is symmetric with respect to  $P$ , thus providing, as the step length goes to zero, a homogenized energy of the form:

$$\mathcal{E}[\nabla\chi(P), \nabla\chi(P) - \nabla\nabla\chi(P)].$$

Of course the identification of the explicit evolution law (or of the Lagrangian) for a system, continuous in both spatial and time variables, which is equivalent to our swarm is not trivial, mostly because of the delicate role played by the fictitious boundary and by the virtual configurations; its characterization will be the object of future investigations.

A further generalization one can consider concerns the introduction of a multiple set of leaders. Indeed, one can impose a family of motions  $\mathcal{M}_\alpha (\alpha = 1, \dots, N)$  to a set of  $N$  selected leaders  $\varrho_1, \dots, \varrho_N$ . Every one of them can be considered as an individual leader to which a set of actual configurations  $C^{t_m}(\varrho_\alpha)$  is associated. We can then define the actual configurations  $C^{t_m}$  relative to the whole set of leaders by simply superposing the effects, i.e. as those

in which the displacement  $\mathbf{u}(i,j)$  of a generic element  $(i,j) \in \mathfrak{S} \setminus \{\varrho_1, \dots, \varrho_N\}$  is the vector sum of the displacements  $\mathbf{u}_\alpha(i,j)$  it has due to the interaction with every single leader

$$\mathbf{u}(i,j) = \sum_{\alpha=1}^N \mathbf{u}_\alpha(i,j)$$

and since the computation of the centroid is a linear operation (in the full set of coordinates of the points) and the concept of first neighbors is Lagrangian in our model, the superposition defined in this way is well-posed. However many features of the considered system, (and in particular the presence of a fictitious boundary at a fixed distance and the evolution through virtual configurations, which weakens the effect of an imposed action as the distance with the leaders increases) make the overall evolution of the system non-linear, which is particularly desirable if one wants to describe the behavior of deformable bodies also in case of large deformations (see below, Fig. 7).

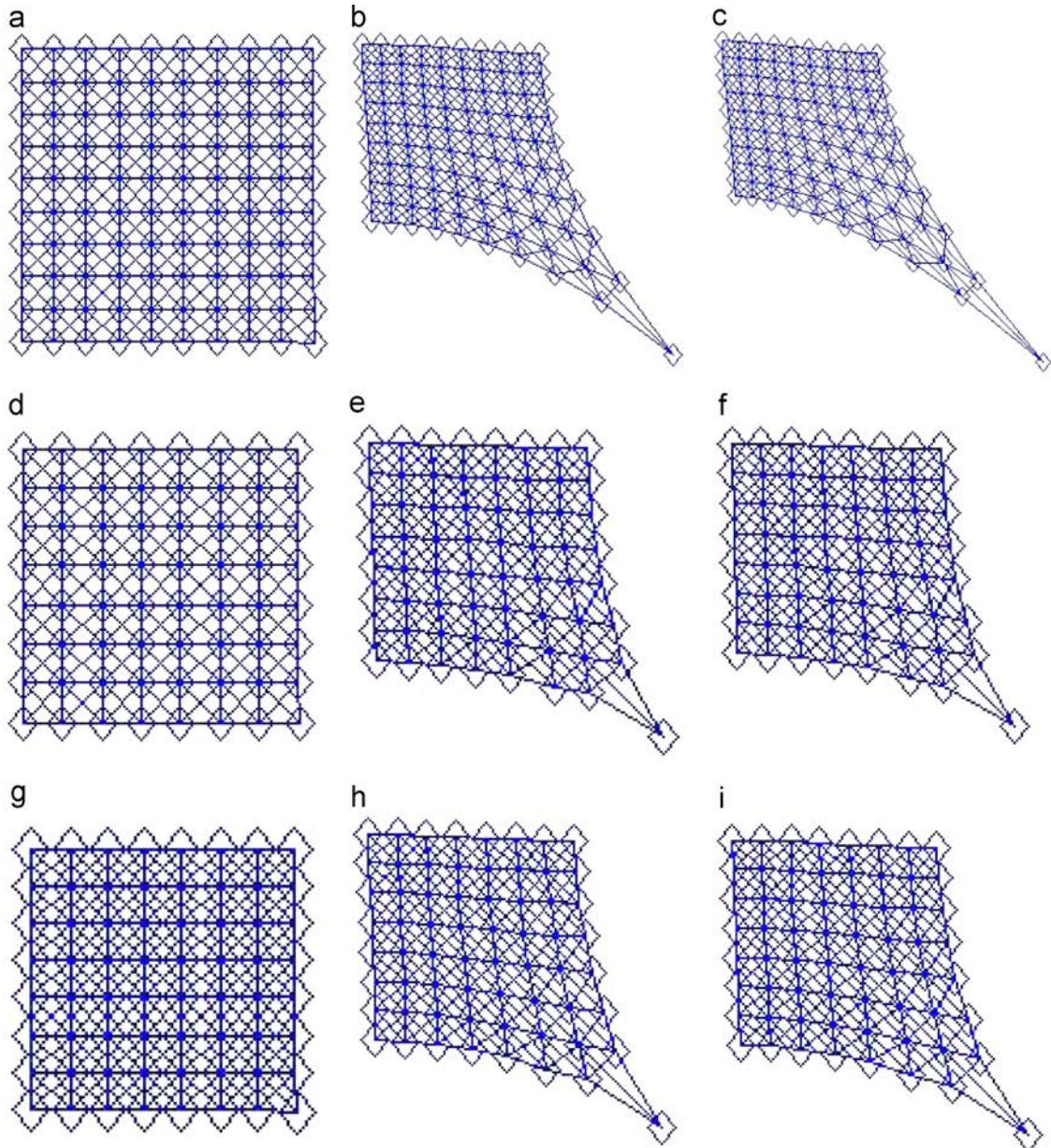


**Fig. 6.** Snapshots of the swarm at time steps  $t=1, 200, 400$  in the case of FNI (a,b,c), SNI (d,e,f) and MI (g,h,i), with the leader moving at velocity  $v=0.05$  length units/time step in direction  $(1, -1)$ .

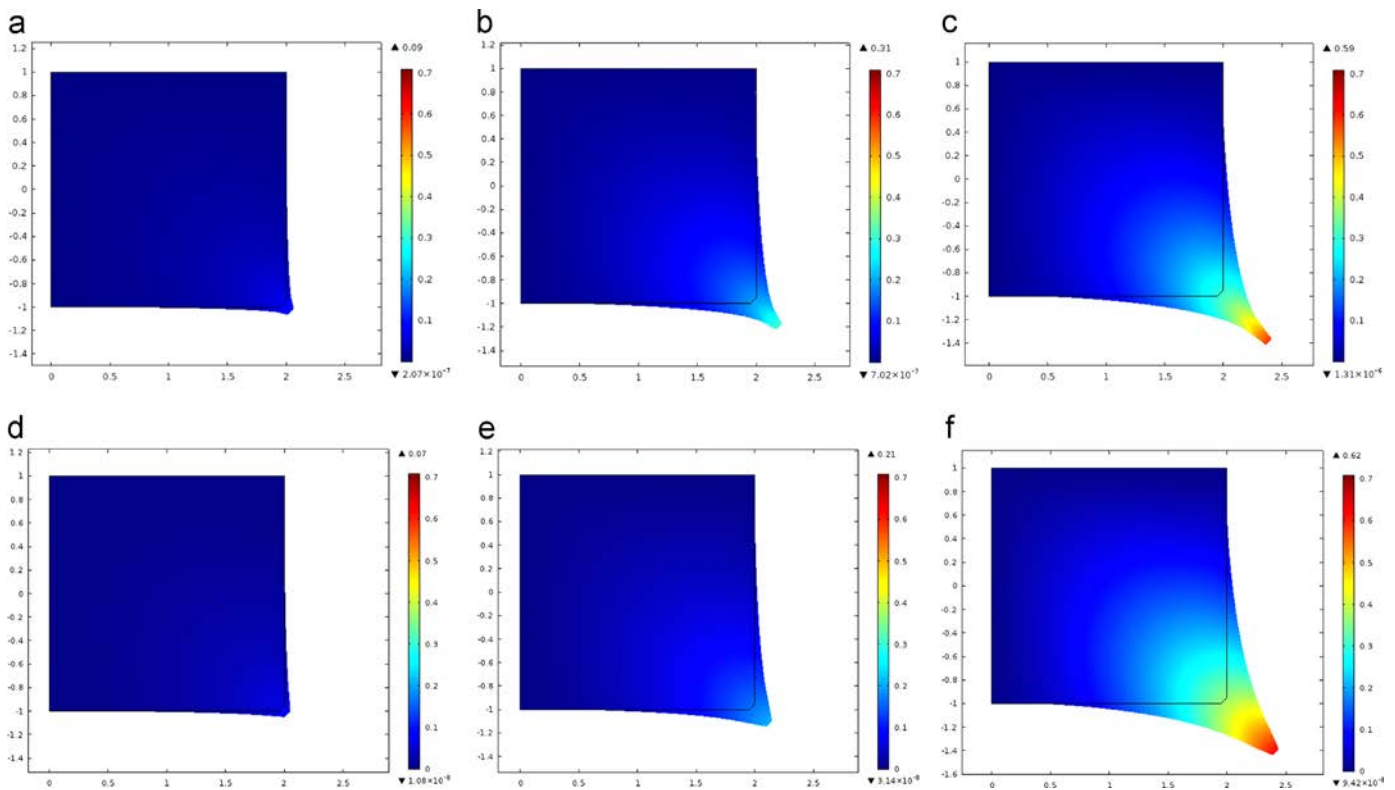


**Fig. 7.** Three snapshots of a continuum square body with an imposed motion on the right bottom vertex in direction  $(1, -1)$ , in the case of a first gradient energy (a,b,c) and a second gradient energy (d,e,f). Colors represent deformations values. (For interpretation of the references to color in this figure caption, the reader is referred to the web version of this paper.)

The formal environment above described allows great flexibility in the choice of the leaders. If one is interested in the comparison between the discrete swarm robot model and its continuous limit, seen as a model for deformable bodies, this means that it is possible to consider a concentrated action (one single leader), a surface line action (leaders belonging to a side), a volume action (leaders belonging to a cluster), or some more exotic mixed cases. Moreover, the interaction can always be introduced as relative to first neighbors, second neighbors or both. Finally, one has to note that the model described is intrinsically dynamic. Indeed, with the evolution procedure before described, in every actual configuration no one of the elements exactly lies in the centroid of its neighbors, which, thinking to the energy we were referring above, means that the evolution is not quasistatic.

In the following section, a numerical investigation of some interesting examples will be provided. In the following numerical simulations, we will focus on leaders belonging to the boundary, since this is the most natural choice for simulating a contact external action. One important point to notice in this connection is that you can perturb the whole system by simply imposing a prescribed motion to boundary elements, independently of the number of elements of the swarm; this feature corresponds, when thinking to the continuous limit, to the simple fact that one can deform a continuum applying an external action to its boundary. The proposed numerical study is of course just a first step in this direction, and further study will be devoted to cases in which the leaders do not belong to the boundary and have more general prescribed motions.

### 3. Numerical simulations

We considered three interaction laws for our numerical investigation, namely a pure first neighbor interaction (FNI), a pure

second neighbor interaction (SNI), and a mixed one<sup>5</sup> (MI). As already said, the given set of simulations is intended as a starting dataset, and it should be enlarged and deepened in future investigations. In particular, larger sets of elements have to be taken into account and higher order interactions have to be considered. In this connection, one has to note that the presence of highly non-local interactions could need the use of complex elements in order to suitably apply a Finite Element Method. Recent results concerning isogeometric finite elements could be of use (see e.g. [14–18]). Moreover, the introduction of more complicated interaction laws, which would be interesting to broaden the set of continuous cases one can approximate, can easily lead to the onset of instabilities in the considered kind of systems, which can be nowadays addressed by means of strong theoretical results available in recent relevant literature (see e.g. [35,22–25]).

In our first group of numerical simulations we chose the bottom right vertex as the leader  $\varrho$ . We considered a set  $\mathfrak{X}_m$  such that the time step is uniform, and imposed to the leader a uniform motion with velocity  $v$  oriented along the direction  $(1, -1)$ . In Fig. 5 we chose  $v=0.01$  length units/time step. The three rows show the evolution with (from top to bottom), FNI, SNI and MI. In every row, the snapshots relative to time steps 1, 500 and 1000 are plotted.

In every case a rather localized elastic-like deformation of the system is visible. It is immediately observable a significant difference between the effect of a FNI with respect to SNI and MI, as in the first case the deformation is much more significant, which closely recalls the effect of the addition of a second gradient deformation energy term to an ordinary first gradient continuum

<sup>5</sup> We recall that by “mixed interaction” we mean the case in which the centroid is computed on the whole set of first and second neighbors as a simple average on the coordinates.

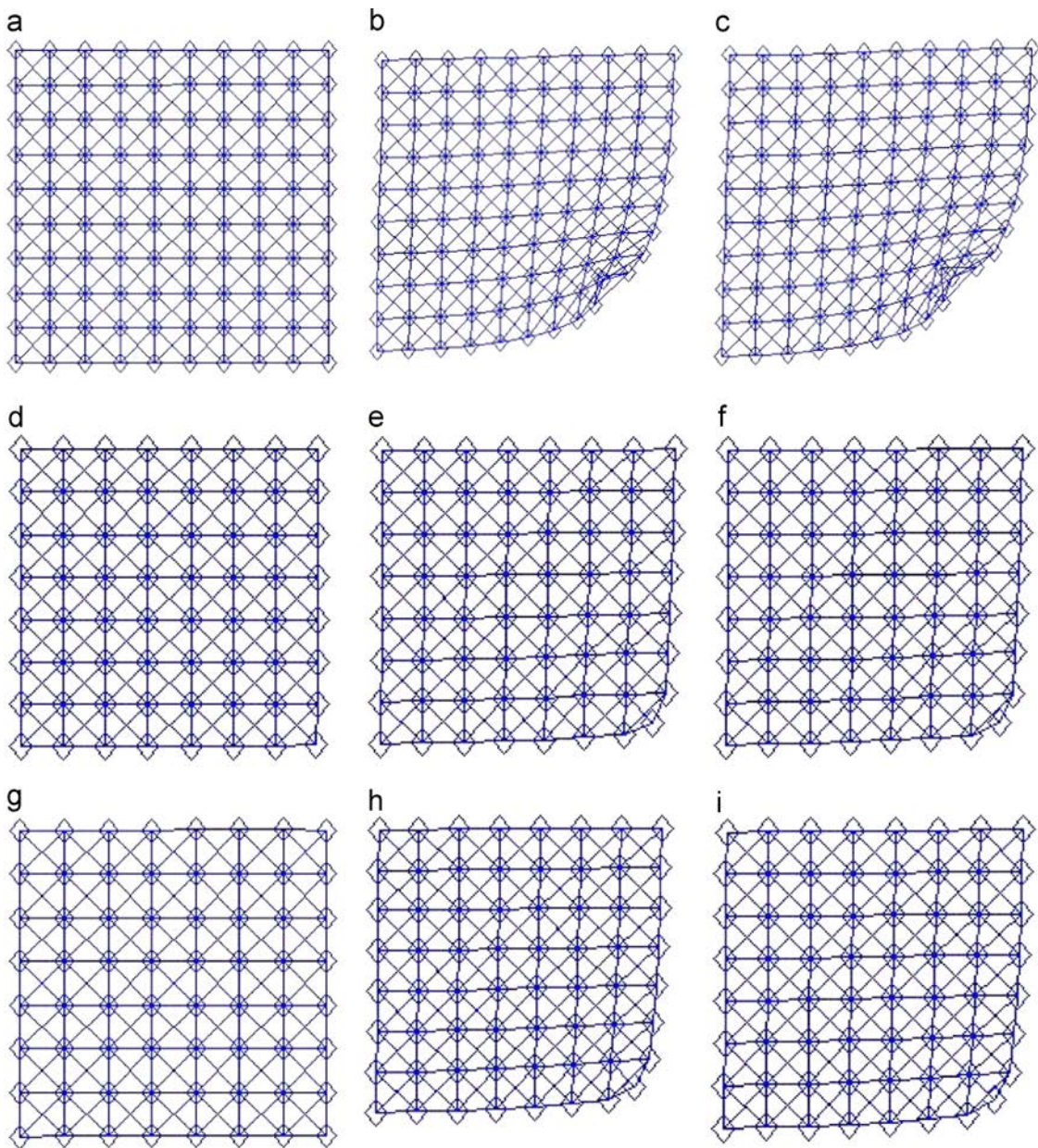


**Fig. 8.** Snapshots of the swarm at time steps  $t=1, 500, 1000$  in the case of FNI (a,b,c), SNI (d,e,f) and MI (g,h,i), with the leader moving at velocity  $v=0.01$  length units/time step in direction  $(-1, 1)$ .

model (see below for a comparison). As one can see comparing the second and the third files (relative to time steps 500 and 1000), there is practically no change in the deformation in the second half of the evolution of the system, which suggests that it asymptotically converges to a limit configuration.

In Fig. 6 the same simulation was performed with a velocity  $v=0.05$  length units/time step, and the snapshots relative to time steps 1, 200 and 400 are plotted. The qualitative behavior of the system is the same as the previous simulation, with the difference that the increased velocity makes the deformation sharper. Also in this case the comparison between second and third files shows that the system seems to asymptotically converge to a limit configuration. With this value for the velocity, a small difference is observable between SNI and MI, with the latter being slightly more deformed, as expected from pure second gradient continuum models.

To allow a direct comparison, we also performed some simulations relative to the behavior of a deformable continuous square

body, which are shown in Fig. 7. Geometric non-linearities for both first and second gradient case were introduced (to account for large deformations), and the form of the energy was the standard one in first gradient case, while it was the one introduced by Mindlin in its general form in [20] for second gradient models, i.e.:  $U(G_{ij}, G_{ij,h}) = \frac{1}{2}G_{ii}G_{ij} + \mu G_{ij}G_{ij} + 4\alpha_1 G_{aa,b}G_{bc,c} + \alpha_2 G_{aa,b}G_{cc,b} + 4\alpha_3 G_{ab,a}G_{cb,c} + 2\alpha_4 G_{ab,c}G_{ab,c} + 4\alpha_5 G_{ab,c}G_{ac,b}$ , where  $G_{ij}$  is the non-linear Green–Saint Venant strain tensor.

The following material parameters were chosen:

$$L = 2 \text{ m}, \quad \mu = 10 \text{ MPam}, \quad \lambda = 15 \text{ MPam}, \quad \rho = 10^5 \text{ kg/m}^2 \\ \alpha_1 = El_m^2, \quad \alpha_2 = El_m^2, \quad \alpha_3 = 2El_m^2, \quad \alpha_4 = El_m^2, \quad \alpha_5 = \frac{1}{2}El_m^2, \quad l_m = 10 \text{ cm}$$

where  $L$  is the side-length,  $\lambda$  and  $\mu$  are Lamé coefficients,  $\rho$  is the density,  $\alpha_i$  are second gradient constitutive parameters,  $E$  the generalized Young modulus, and  $l_m$  a characteristic length (notice that the ratio between the side of the sample and this length is of

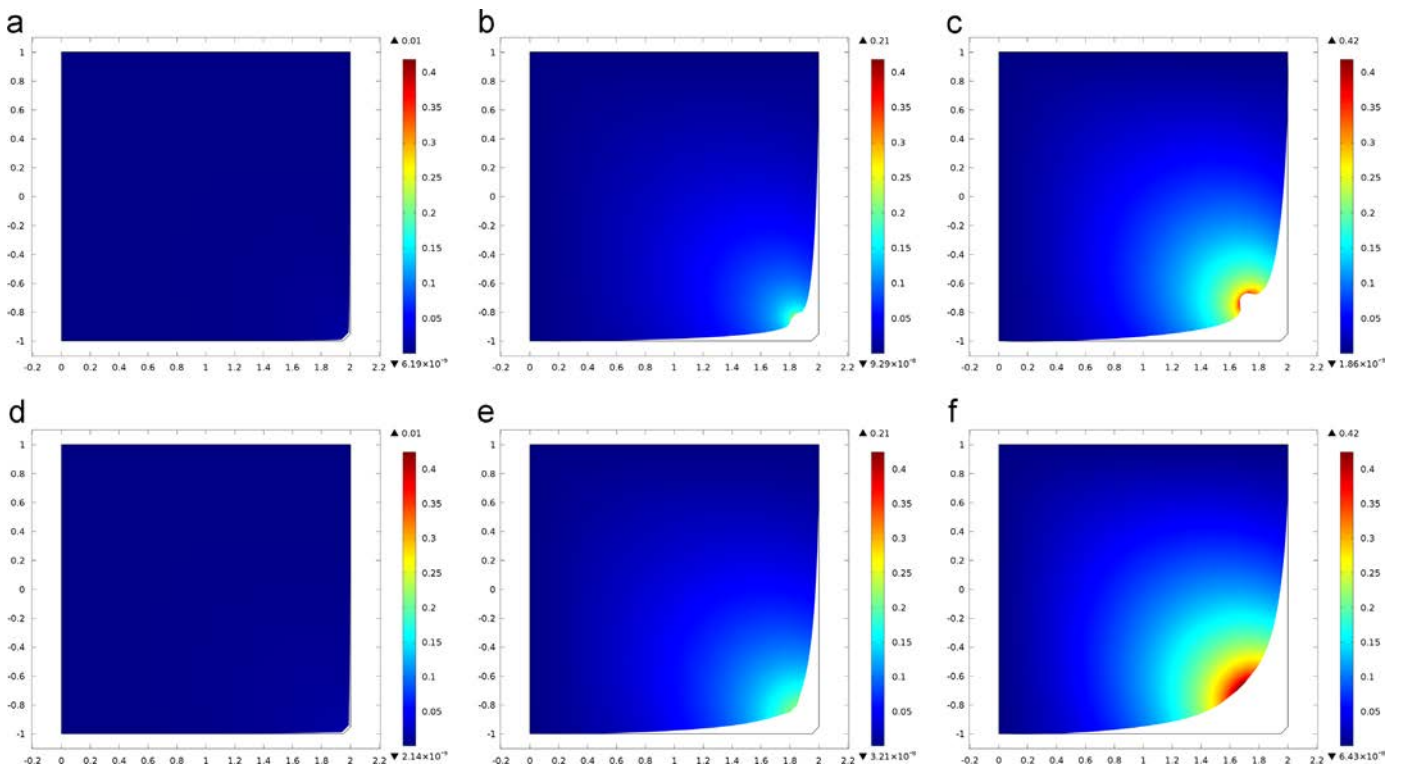


**Fig. 9.** Three snapshots of a continuum square body with an imposed motion on the right bottom vertex in direction  $(-1, 1)$ , in the case of a first gradient energy (a,b,c) and a second gradient energy (d,e,f). Colors represent deformations values. (For interpretation of the references to color in this figure caption, the reader is referred to the web version of this paper.)

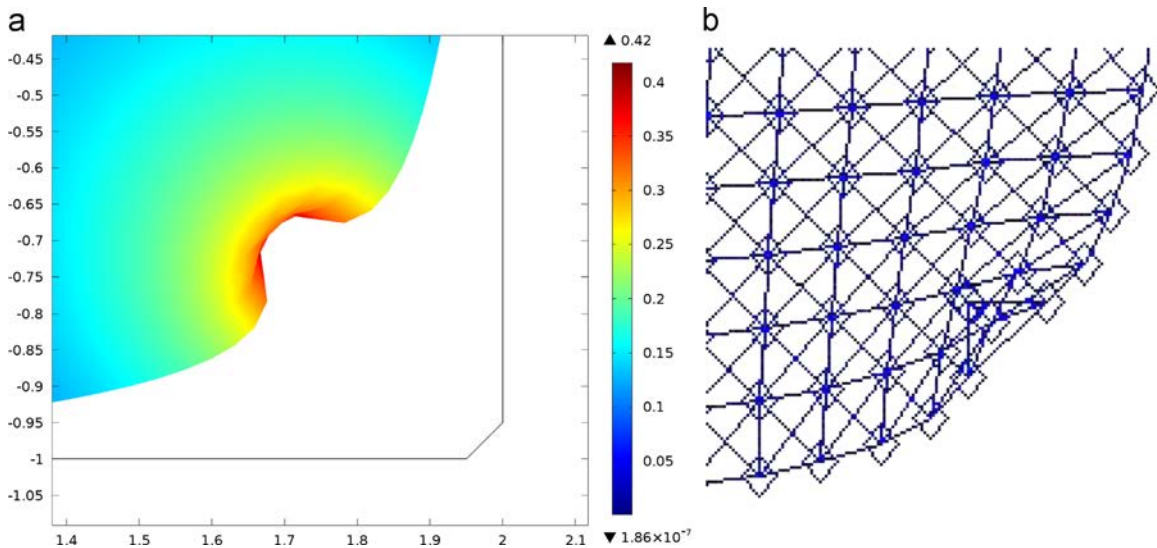


**Fig. 10.** Comparison of first gradient energy (a) and FNI (b) in the case of an imposed motion in direction  $(-1, 1)$ . Note the loss of convexity around the vertexes in both cases.

the same order of magnitude of the ratio between the lattice step and the side of the swarm in the initial configuration). A prescribed uniform motion, with velocity oriented along the direction  $(1, -1)$ , is imposed to the points belonging to the base of a small triangular region symmetrically cut off from the body around the bottom right vertex. The two panels refer to the cases of a first gradient (above) and second gradient (below) continuum model, and the total displacement is shown by means of a color map. As one can see, the type of deformation which one observes in the two cases is very similar to what seen before with (respectively) FNI and SNI/MI.

In the next simulation we inverted the motion of the leader  $\Omega$ , imposing to it a uniform motion along the direction  $(-1, 1)$  with velocity  $v=0.01$  length units/time step, i.e. “pushing” the system rather than “pulling” it. In Fig. 8 the snapshots relative to time steps 1, 500 and 1000 are plotted, and the three rows respectively show FNI, SNI and MI. Also in this case the system is much less deformed in the last two cases.

Even in this case we performed a continuum simulation to allow a direct comparison. In the simulation shown in Fig. 9 the same energy and constitutive parameters before mentioned were used. A prescribed uniform time-dependent displacement along

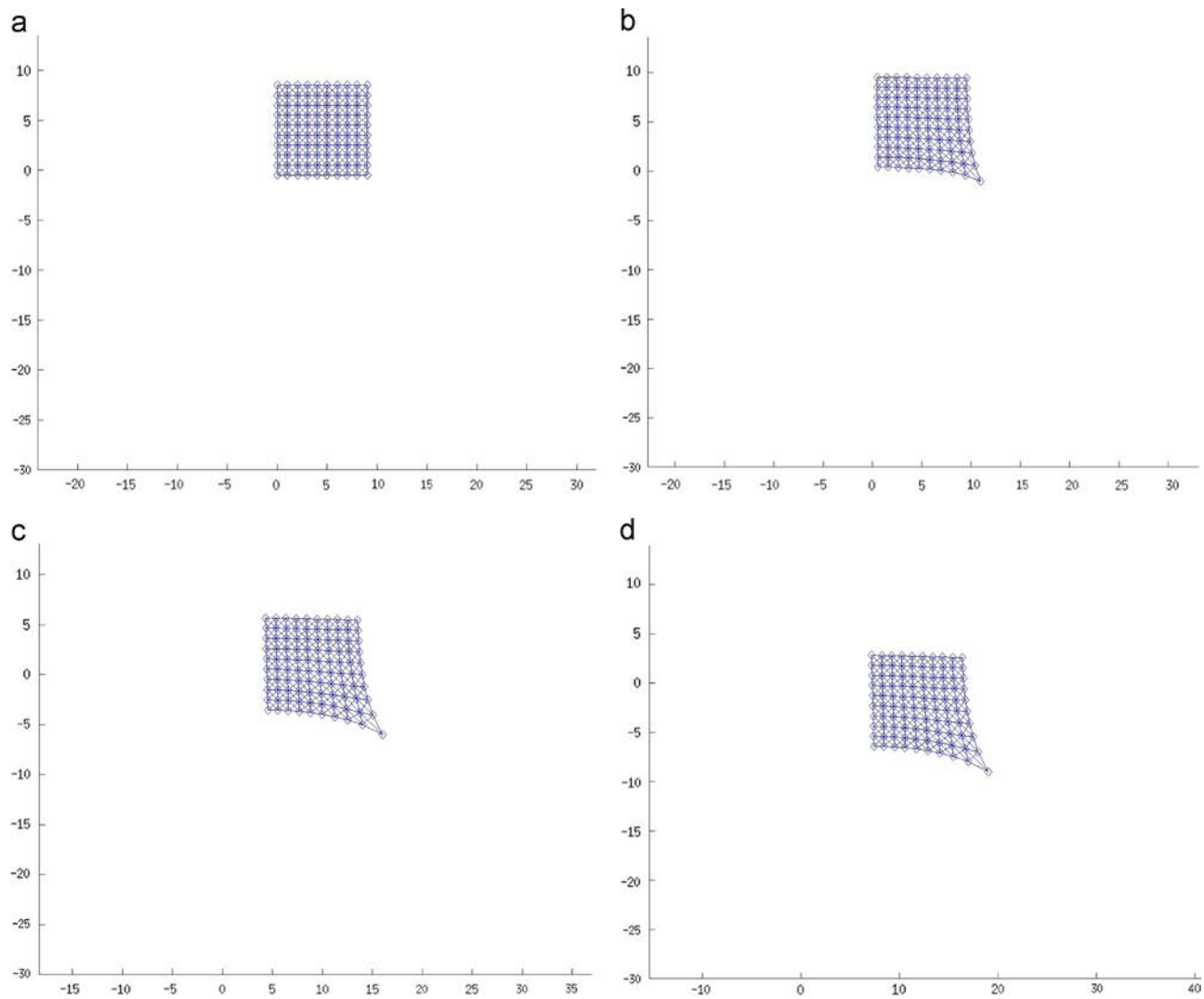


**Fig. 11.** Translation of the swarm. Snapshots of the swarm at time steps  $t = 1, 200, 700, 1000$  in the case of FNI, with the leader moving at velocity  $v = 0.01$  length units/time step in direction  $(1, -1)$ .

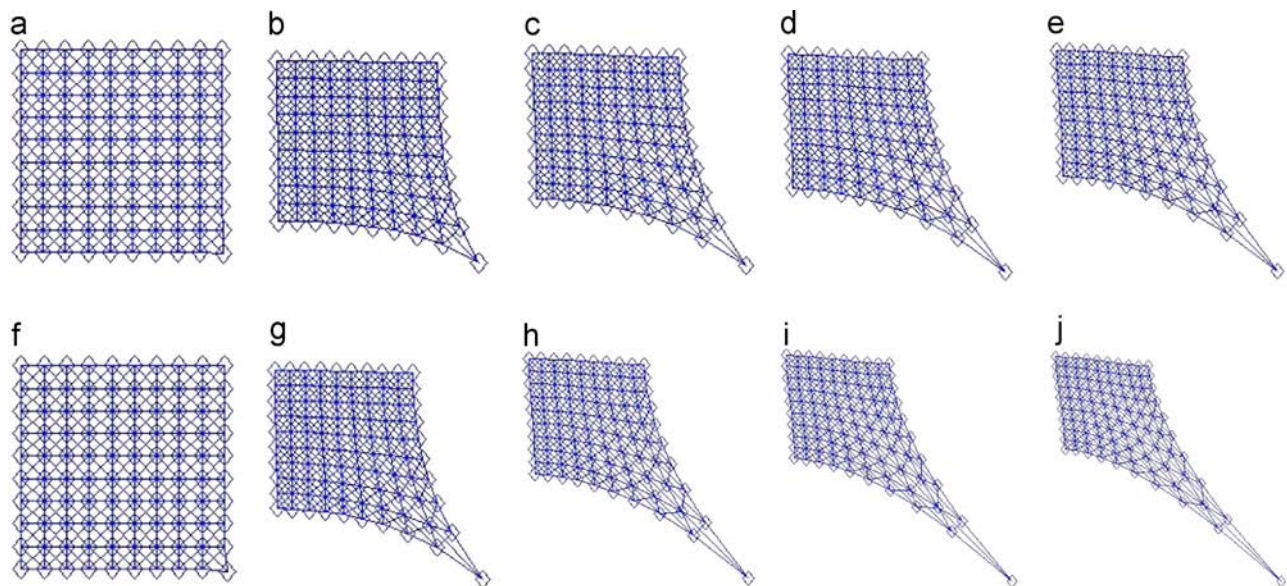


**Fig. 12.** Snapshots of the swarm at time steps  $t = 1, 50, 100, 150, 200$  in the case of FNI, with the leader moving at velocity  $v = 0.05$  length units/time step (a,b,c,d,e) and at velocity  $v = 0.1$  length units/time step (f,g,h,i,j) (both in direction  $(-1, 1)$ ).

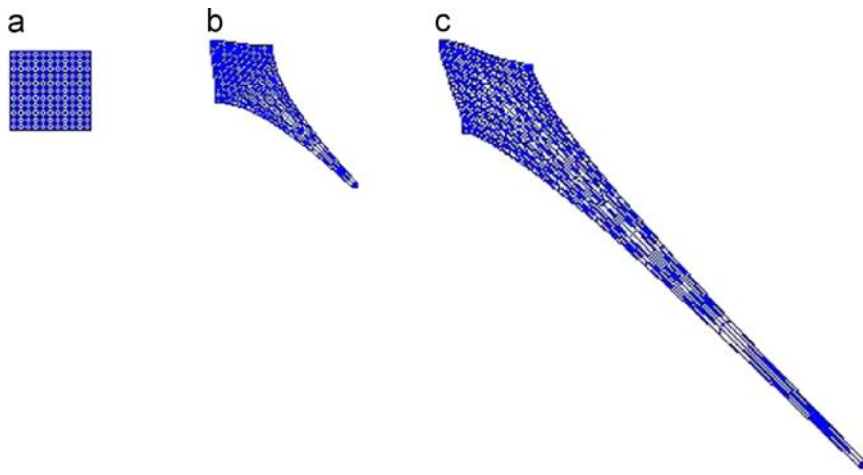


**Fig. 13.** Snapshots of the swarm at time steps  $t=1,200,400$  in the case of FNI, with the leader moving at time varying velocity with acceleration  $a=0.01$  length units/squared time step (both the initial value  $v_0$  and  $a$  in direction  $(1, -1)$ ).

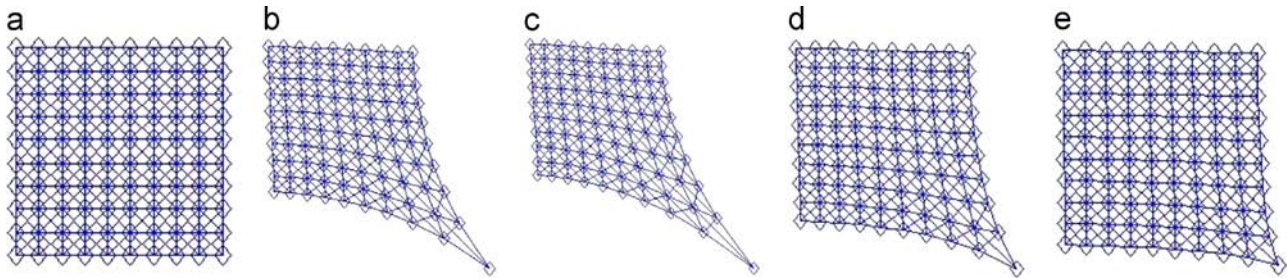


**Fig. 14.** Snapshots of the swarm at time steps  $t=1,250,500,750,1000$  in the case of FNI, with the leader moving at velocity  $v=0.03$  length units/ time step in direction  $(1, -1)$  up to  $t=500$ , and  $v=0$  length units/ time step for  $500 \leq t \leq 1000$ .

the direction  $(-1, 1)$  was imposed to the points belonging to the base of a small triangular region symmetrically cut off from the body around the bottom right vertex, and the total displacement is shown by means of a color map. The two rows are relative to first gradient (above) and second gradient (below) models. As you can see, the overall behavior closely resembles what was observed in the analogous discrete simulation, as the local deformation is much sharper in first gradient/first neighbor case. Moreover, a close relationship concerning some further details of the deformation can be shown. In Fig. 10, a zoom of the two bottom right vertexes is shown concerning the simulations plotted in Fig. 8 (FNI, last snapshot) and Fig. 9 (first gradient). As one can observe, a significant loss of convexity is visible in both cases around the area in which the displacement is imposed, while no such effect is there when considering a second gradient/SNI case.

In the following figure the reference axes are also plotted, so as to be able to evaluate, besides the deformation, the translation motion of the system. In Fig. 11 the snapshots relative to time steps 1, 200, 700 and 1000 are plotted in case of a velocity  $v=0.01$  length units/time step directed along  $(1, -1)$ . It is interesting to note that in the second snapshot there is practically no translation still (as one can see observing the points belonging to the upper side), while a significant translation of the whole system is visible in the last two snapshots. This suggests the existence of a critical time (depending on the velocity of the leader) after which overall translation becomes appreciable. Moreover, in order to study the limit configuration of the system with different velocities, we considered the comparison between the evolution with two relatively large velocities. In Fig. 12 the two rows refer indeed to two cases with  $v=0.05$  (above) and  $0.1$  (below) length units/time step, and the snapshots relative to time steps 1, 50, 100, 150 and

200 are plotted. One can observe that in the limit configuration the two sides intersecting in the upper left vertex form a characteristic angle  $\theta$ , which was very close to 90 degrees in case of  $v=0.01$  (see Fig. 5), and is progressively decreasing with higher velocities.

To further investigate the behavior of the angle  $\theta$ , we considered in the next simulation the case in which the leader  $\varrho$  has a uniformly accelerated motion ( $a=0.01$  length units/squared time step,  $v_0=0.01$  length units/time step), again in direction  $(1, -1)$ . The result is plotted in Fig. 13 (snapshots corresponding to  $t=1, 200, 400$ ). The angle  $\theta$  in this case does not seem to converge to a non-zero value, and it keeps decreasing in all the time interval we considered (up to  $t=1000$ ).

Another case we considered is the one in which the leader  $\varrho$  has an imposed motion which is uniform with velocity  $v=0.03$  length units/time step up to time step  $t=500$ , and then is set to 0 up to time step  $t=1000$ . The result is shown in Fig. 14, where snapshots relative to time steps  $t=1, 250, 500, 750$  and 1000 are plotted. As you can see, in the second half of the time interval, the system tends to return to its original configuration, which is a basic characteristic of the behavior of elastic deformable bodies. Moreover, it should be pointed out that the system actually does not reach the initial configuration at any given time, but instead converges again asymptotically to it. This behavior, on the whole, resembles typical effects related to combined inertia and friction, which is particularly interesting since in the model no explicit terms accounting for the mass or of dissipation were introduced, and the overall behavior observed was just a consequence of the assumed interaction law.

Finally, in the following group of simulations we considered the case in which there are two leaders  $\varrho_1, \varrho_2$ . Two opposite vertexes were chosen as the leaders and the two motions have opposite

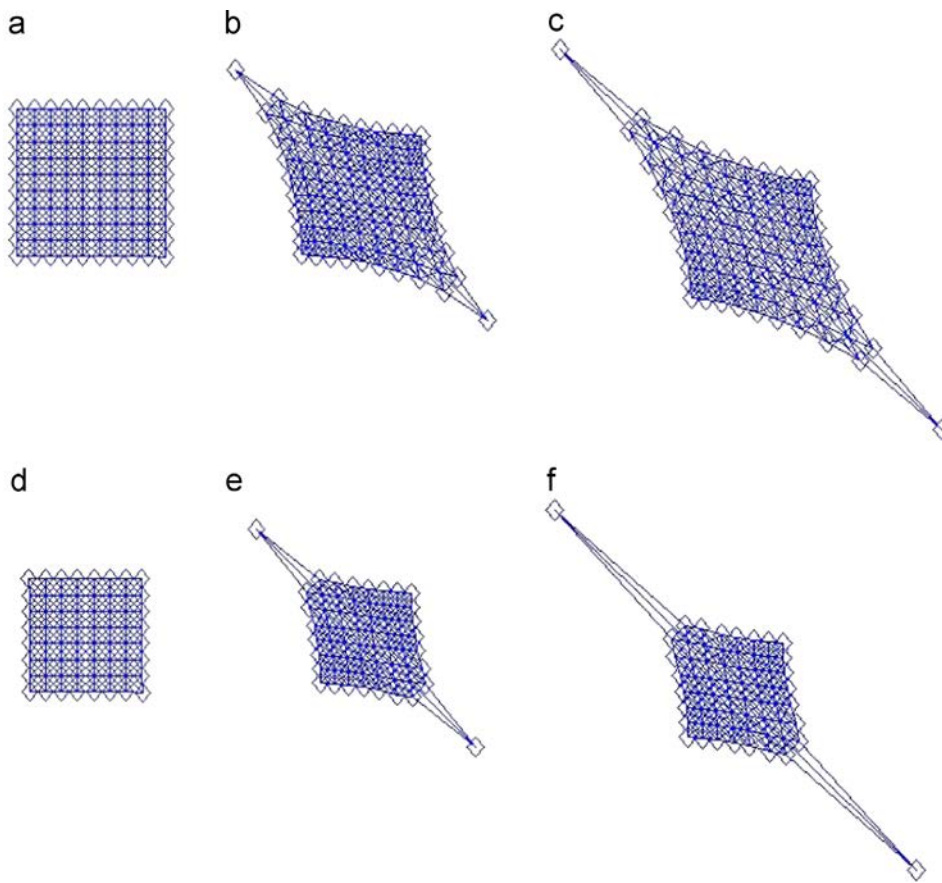


**Fig. 15.** Snapshots of the swarm at time steps  $t=1,100,200$  in the case of FNI (a,b,c) and MI (d,e,f), with two leader moving at velocity  $v=0.05$  length units/ time step (the two vertexes are moving in opposite directions).

directions,  $(1, -1)$  for the bottom right vertex and  $(-1, 1)$  for the upper left one. The velocity was set to 0.05 length units/time step, and the two rows refer to the FNI (above) and MI (below). In Fig. 15 one can see that the system has a more compact shape in this second case, while the leader tends to be more sharply out-distanced. This too recalls what happens in second gradient continuum models.

Let us conclude this section by pointing out that, computationally speaking, the proposed algorithm seems very promising. Indeed, the computational cost is in our case more or less just linear in the number of elements of the swarm, which is not the case with either FEM or FDM with respect to, respectively, the number of mesh elements or of nodes considered. This means that the size limit for this kind of systems allowed by the current computational power is very high.

#### 4. Conclusions

Our work intended to show and discuss some similarities between a simple discrete system and continuous deformable bodies. The study of discrete systems as a tool for improving our understanding and our possibility of numerical control over continuous deformable bodies is a well-established research area (the reader can see, for instance, [29,30,26–28]) which is particularly vital nowadays thanks to the great recent development of numerical tools and methods. The increasing interest in nanotechnologies, in particular, is leading to a great development of works in which both a continuous and a discrete formulation are used in the same framework (see e.g. the cases analyzed in [34,32,31,33]).

The set of numerical results provided in the present paper justify the claim that the simple robotic system model here described is a promising theoretical tool for discrete approximation of continuum deformable bodies having a generalized deformation energy. What is attractive in the proposed model, in our opinion, is its great simplicity and the flexibility it allows in the choice of the kind of considered interaction and imposed contact actions. Moreover, the evolution process via the definition of virtual configurations above described seems suitable to reproduce some characteristic effects of both deformation and inertia/friction. Indeed, the presence of a critical time after which overall translation begins, and the fact that the system seems to verify some basic properties one should expect from a discrete model of elastic (or in general deformable) bodies, are very promising characteristics that makes further investigation on the subject particularly interesting. Moreover, besides general resembling, some rather specific characteristic (like the loss of convexity in the boundary only seen in FNI with the same imposed “pushing” displacement) that clearly distinguish first and second gradient continuum models are observable in the comparison between FNI and SNI in our simulations.

The ways in which the proposed model can be enriched/generalized are many. One can indeed consider, as said, more complex interactions, e.g. cases in which the interaction is suitably weighted by the local density, the distance, some kind of directionality or other characteristics. While it is reasonable to conjecture that the continuous limit of the system considered herein is a higher order continuum model, in case of an enriched interaction a micromorphic approach, which is a natural generalization of the previously mentioned type of models, is probably the most suitable theoretical tool (on the subject a classical

reference is [42]; for a relevant sample of the existing literature on micromorphic continua the reader can see e.g. [13,38,45,44,46]). The degree of interest towards micromorphic continua is today very high and increasing, also due to the desire to describe and design new complex metamaterials (for a review on metamaterials and their modeling through micromorphic/microstructured continua the reader can see [39] and as examples of homogenised microstructured continua [40,41]) The possibility to describe, by means of interaction laws between relatively “few” discrete elements, the characteristics that in micromorphic continua are represented via additional kinematic descriptors (which are in general at least piece-wise continuous functions) looks very interesting, especially for the potential effect on the computational cost of related numerical software.

Further investigations covering both theoretical and numerical aspects of the robotic system model presented here, which as we saw can potentially concern various different research areas, promise to be of great interest.

## Acknowledgments

The authors thank the PRIN “Dynamics, stability and control of flexible structures” of the Italian Ministry of Education, Universities and Research for having funded this research.

## References

- [1] E. Sahin, *Swarm robotics: from sources of inspiration to domains of application*, Swarm Robotics, Springer, Berlin, Heidelberg (2005) 10–20.
- [2] E. Sahin, W.M. Spears, A.F. Winfield (Eds.), *Swarm Robotics*, in: Second SAB 2006 International Workshop, Rome, Italy, September 30–October 1, 2006, Revised Selected Papers, vol. 4433, Springer Science & Business Media, Berlin, Germany, 2007.
- [3] M. Brambilla, E. Ferrante, M. Birattari, M. Dorigo, *Swarm robotics: a review from the swarm engineering perspective*, *Swarm Intell.* 7 (1) (2013) 1–41.
- [4] V. Gazi, On Lagrangian dynamics based modeling of swarm behavior, *Physica D: Nonlinear Phenom.* 260 (2013) 159–175.
- [5] Y. Liu, K.M. Passino, M. Polycarpou, Stability analysis of one-dimensional asynchronous swarms, *IEEE Trans. Autom. Control* 48 (10) (2003) 1848–1854.
- [6] A. Adamatzky, J. Jones, Towards Physarum robots: computing and manipulating on water surface, *J. Bionic Eng.* 5 (4) (2008) 348–357.
- [7] S. Tsuda, K.P. Zauner, Y.P. Gunji, Robot control with biological cells, *Biosystems* 87 (2) (2007) 215–223.
- [8] J. Jones, A. Adamatzky, Towards Physarum binary adders, *Biosystems* 101 (1) (2010) 51–58.
- [9] J.M. Miller, A Whole Greater than the Sum of its Parts: Mathematically Modeling and Analyzing Swarms, University of Delaware, Newark, New Jersey, 2012.
- [10] S. Berman, Á. Halász, V. Kumar, S. Pratt, *Algorithms for the analysis and synthesis of a bio-inspired swarm robotic system*, *Swarm Robotics*, Springer, Berlin, Heidelberg (2007) 56–70.
- [11] C. Pideri, P. Peppcher, A second gradient material resulting from the homogenization of an heterogeneous linear elastic medium, *Contin. Mech. Thermodyn.* 9 (5) (1997) 241–257.
- [12] G. Rosi, I. Giorgio, V.A. Eremeyev, Propagation of linear compression waves through plane interfacial layers and mass adsorption in second gradient fluids, *ZAMM-J. Appl. Math. Mech./Z. Angew. Math. Mech.* 93 (12) (2013) 914–927.
- [13] J. Altenbach, H. Altenbach, V.A. Eremeyev, On generalized Cosserat-type theories of plates and shells: a short review and bibliography, *Arch. Appl. Mech.* 80 (1) (2010) 73–92.
- [14] M. Cuomo, L. Greco, Isogeometric Analysis of Space Rods: Considerations on Stress Locking, 2012.
- [15] M. Cuomo, L. Contrafatto, L. Greco, A variational model based on isogeometric interpolation for the analysis of cracked bodies, *Int. J. Eng. Sci.* 80 (2014) 173–188.
- [16] L. Greco, M. Cuomo, Multi-patch isogeometric analysis of space rods, in: *YIC*, 2012, pp. 24–27.
- [17] L. Greco, M. Cuomo, B-Spline interpolation of Kirchhoff-Love space rods, *Comput. Methods Appl. Mech. Eng.* 256 (2013) 251–269.
- [18] A. Cazzani, M. Malagù, E. Turco, Isogeometric analysis of plane-curved beams, *Math. Mech. Solids* (2014) 1081286514531265.
- [19] V. Gazi, K.M. Passino, *Swarm Stability and Optimization*, Springer Science and Business Media, Berlin, Germany, 2011.
- [20] R.D. Mindlin, *Micro-structure in Linear Elasticity*, Department of Civil Engineering Columbia University New York 27, New York, 1964.
- [21] L. Placidi, G. Rosi, I. Giorgio, A. Madeo, Reflection and transmission of plane waves at surfaces carrying material properties and embedded in second-gradient materials, *Math. Mech. Solids* (2013) 1081286512474016.
- [22] A. Luongo, G. Piccardo, Linear instability mechanisms for coupled translational galloping, *J. Sound Vib.* 288 (4) (2005) 1027–1047.
- [23] A. Luongo, D. Zulli, G. Piccardo, Analytical and numerical approaches to non-linear galloping of internally resonant suspended cables, *J. Sound Vib.* 315 (3) (2008) 375–393.
- [24] A. Luongo, D. Zulli, Aeroelastic instability analysis of NES-controlled systems via a mixed multiple scale/harmonic balance method, *J. Vib. Control* (2013) 1077546313480542.
- [25] A. di Egidio, A. Luongo, A. Paolone, Linear and non-linear interactions between static and dynamic bifurcations of damped planar beams, *Int. J. Non-Linear Mech.* 42 (1) (2007) 88–98.
- [26] F. dos Reis, J.F. Ganghoffer, Discrete homogenization of architected materials: implementation of the method in a simulation tool for the systematic prediction of their effective elastic properties, *Tech. Mech.* 30 (2010) 85–109.
- [27] F. dos Reis, J.F. Ganghoffer, Construction of micropolar continua from the homogenization of repetitive planar lattices, *Mechanics of generalized continua*, Springer, Berlin, Heidelberg (2011) 193–217.
- [28] M. Assidi, F. dos Reis, J.F. Ganghoffer, Equivalent mechanical properties of biological membranes from lattice homogenization, *J. Mech. Behav. Biomed. Mater.* 4 (8) (2011) 1833–1845.
- [29] I. Goda, M. Assidi, S. Belouettar, J.F. Ganghoffer, A micropolar anisotropic constitutive model of cancellous bone from discrete homogenization, *J. Mech. Behav. Biomed. Mater.* 16 (2012) 87–108.
- [30] F. dos Reis, J.F. Ganghoffer, Equivalent mechanical properties of auxetic lattices from discrete homogenization, *Comput. Mater. Sci.* 51 (2012) 314–321.
- [31] V.A. Eremeyev, E.A. Ivanova, N.F. Morozov, S.E. Strohkov, The spectrum of natural oscillations of an array of micro- or nanospheres on an elastic substrate, *Dokl. Phys.* 52 (12) (2007) 699–702.
- [32] V.A. Eremeyev, E.A. Ivanova, N.F. Morozov, A.N. Soloviev, Method of determining the eigenfrequencies of an ordered system of nanoobjects, *Tech. Phys.* 52 (1) (2007) 1–6.
- [33] V.A. Eremeyev, E.A. Ivanova, D.A. Indeitsev, Wave processes in nanostructures formed by nanotube arrays or nanosize crystals, *J. Appl. Mech. Tech. Phys.* 51 (4) (2010) 569–578.
- [34] V.A. Eremeyev, E.A. Ivanova, N.F. Morozov, A.N. Soloviev, On the determination of eigenfrequencies for nanometer-size objects, *Dokl. Phys.* 51 (2) (2006) 93–97.
- [35] V.A. Eremeyev, A.B. Freidin, L.L. Sharipova, Non-uniqueness and stability in problems of the equilibrium of elastic two-phase solids, *Dokl. Ross Akad. Nauk.* 391 (2) (2003) 189–193.
- [36] I. Giorgio, A. Culla, D. del Vescovo, Multimode vibration control using several piezoelectric transducers shunted with a multiterminal network, *Arch. Appl. Mech.* 79 (9) (2009) 859–879.
- [37] G. Rosi, I. Giorgio, V.A. Eremeyev, Propagation of linear compression waves through plane interfacial layers and mass adsorption in second gradient fluids, *ZAMM-J. Appl. Math. Mech./Z. Angew. Math. Mech.* 93 (12) (2013) 914–927.
- [38] U. Andreaus, I. Giorgio, T. Lekszycki, A 2D continuum model of a mixture of bone tissue and bio-resorbable material for simulating mass density redistribution under load slowly variable in time, *ZAMM-J. Appl. Math. Mech./Z. Angew. Math. Mech.* 94 (12) (2014) 978–1000.
- [39] D. del Vescovo, I. Giorgio, Dynamic problems for metamaterials: review of existing models and ideas for further research, *Int. J. Eng. Sci.* 80 (2014) 153–172.
- [40] S. Federico, A. Grillo, Non-Linear Elasticity and Permeability of Fibre-Reinforced Porous Media, *Mechanics of Materials* 44 (2012) 58–71. <http://dx.doi.org/10.1016/j.mechmat.2011.07.010>.
- [41] A. Grillo, S. Federico, G. Wittum, Growth, Mass Transfer, And Remodeling in Fiber-Reinforced, Multi-Constituent Materials, *International Journal of Non-Linear Mechanics* 47 (2) (2012) 388–401. <http://dx.doi.org/10.1016/j.ijnonlinmec.2011.09.026>.
- [42] A.C. Eringen, *Mechanics of Micromorphic Continua*, Springer, Berlin, Heidelberg (1968) 18–35.
- [43] A. Rinaldi, L. Placidi, A microscale second gradient approximation of the damage parameter of quasi-brittle heterogeneous lattices, *ZAMM - Z. Angew. Math. Mech./J. Appl. Math. Mech.* (2013) 94 (10) (2014) 862–877. <http://dx.doi.org/10.1002/zamm.201300028>.
- [44] L. Placidi, K. Hutter, Thermodynamics of polycrystalline materials treated by the theory of mixtures with continuous diversity, *Cont. Mech. Thermodyn.* 17.6 (2006) 409–451.
- [45] L. Placidi, S.H. Faria, K. Hutter, On the role of grain growth, recrystallization and polygonization in a continuum theory for anisotropic ice sheets, *Ann. Glaciol.* 39 (1) (2004) 49–52.
- [46] D. Scerrato, I. Giorgio, A. Madeo, A. Limam, F. Darve, A simple non-linear model for internal friction in modified concrete, *Int. J. Eng. Sci.* 80 (2014) 136–152.
- [47] F. dell’Isola, P. Peppcher, A. Madeo, How contact interactions may depend on the shape of Cauchy cuts in Nth gradient continua: approach “à la D’Alembert”, *Z. Angew. Math. Phys.* 63 (6) (2012) 1119–1141.